Journal of the Korean Nuclear Society
Volume 35, Number 5, pp.471~481, October, 2003

<Technical Note>

Microstructural Characteristics of the Fuel Cladding Tubes Irradiated in Kori Unit 1

H.G. Kim, J.H. Baek, M.H. Lee, Y.B. Chun, and Y.H. Jeong
Korea Atomic Energy Research Institute
150 Dukjin-dong Yuseung-gu, Daejeon 305-353, Korea
yhjeong@kaeri.re.kr

(Received Octomber 15, 2002)

Abstract

In order to evaluate the microstructural characteristics of irradiated fuel claddings (Zircaloy-4), two irradiated specimens having different burnups (18 GWD/MTU and 42 GWD/MTU) were prepared from the G23-M4 fuel rods, which were loaded in Kori Unit 1 for 4 fuel cycles. The oxide thickness, hydride morphology and hardness change were characterized by an optical microscope and a micro-hardness tester after preparing the irradiated specimens in the PIE (Post Irradiation Examination) facilities. The dislocation loops and the amorphous transformation of precipitates induced by the neutron irradiation in the nuclear plant were also examined by a TEM. As the burnup increased from 18 GWD/MTU to 42 GWD/MTU, the oxide thickness increased from 6.0μm to 25.3μm and the contents of hydrogen pick-up in the Zr matrix also greatly increased. In the comparison of the hardness of the unirradiated fuel cladding, the amount of hardness increase was nearly 9.3% and 24.2% for the irradiated samples of 18 and 42 GWD/MTU, respectively. Both <a>-type dislocation loops and <c>-type dislocation components were observed simultaneously in the irradiated specimens and the densities of the dislocation was increased by increasing the burnup. The precipitates in both the irradiated specimens were amorphously transformed by the neutron irradiation and the trend of the amorphous transformation of the precipitates was enhanced at a higher burnup.

Key Words : Zr, fuel cladding, Zircaloy-4, neutron-irradiation, hydride, dislocation loop, amorphous

1. Introduction

Korea is one of the advanced countries that can design and construct nuclear power plants including nuclear fuel assemblies. Especially, the Korea Nuclear Fuel Company (KNFC) constructs, from design to fabrication, nuclear fuel rod assemblies and supplies them to domestic nuclear power plants. Since the price of fuel cladding material is over 50% that of the nuclear fuel rod assembly, it is important to characterize the cladding material and improve its quality in order

to save cost and increase the safety of nuclear power plants. The performance of new cladding tubes developed in advanced countries is being presented based on that of Zircaloy-4. So, it is also important to learn how to analyze and identify the properties of irradiated Zircaloy-4 tube to evaluate the performance of advanced fuel cladding tubes. Some properties of irradiated Zircaloy-4 tube have been studied using TEM in other countries. A lot of the study was focused on the microstructual changes of Zircaloy-4 from its irradiation. When Zircaloy-2 alloy was irradiated with the fluence of 1.5×10^{20} n/cm^2 at 300℃, Buckley[1] suggested that the vacancy loops of <c>-type dislocation formed on basal planes, the interstitial loops of <a>-type loop formed on the prism planes, and the loops size and relative spacing of dislocation was changed by the irradiation temperature. After investigating the irradiation characteristics of Zr-based alloys, D.O. Northood[2,3] reported that they depend on the fluence. He also reported that Zr-based alloys weren' t damaged when they were irradiated under the fluence of $2\sim3 \times 10^{19}$ n/cm^2 (E>1MeV) and the alloys showed black spots or dislocation loops if they were irradiated over the fluence. Griffiths[4-6] observed that interstitial vacancy loops were located along a/3<11$\bar{2}$0> near (10$\bar{1}$0). It is known that there is a close relationship between the formation of the dislocation loops and irradiation growth rate. That is, the irradiation growth takes place along the length of the fuel rod due to the crystallographic anisotropy of the interstitial loops formed in the cladding tube but its mechanism is not yet identified[7,8]. Zr matrix can be damaged by the collision of the neutron beam. The damage can appear as the formation of dislocation loops or precipitates. Since the second phases of Zr-based alloys are very small, their characteristics have not been analyzed as much recently, in detail. It was reported that the precipitates formed in Zircaloy-2 and Zircaloy-4 alloys could be transformed into amorphous structures after irradiation[9,10]. Zr_2(Ni, Fe) and Zr(Cr, Fe)$_2$ precipitates were amorphous microstructures when they have been irradiated with the fluence of 1.0×10^{21} n/cm^2 at 350K. As the precipitate is becoming an amorphous, the chemical potential of Fe in the precipitate will be increased more than that of its neighbor metal thus the precipitate disappears in the end with the Fe element in the precipitate becoming diffused into the matrix. But, compared with the researches on the irradiated cladding tube, much research on the un-irradiated one has been carried out in Korea. Therefore, this research is an attempt to analyze the irradiation characteristics of specimens from the sound Zircaloy-4 cladding tubes, which have been irradiated for 4 cycles in Kori Unit 1, having a burnup history of 18 and 42 GWD/MTU. So, the microstructure of the specimens was analyzed using TEM and their macroscopic structure using the optical microscope and the hardness tester. Hydrogen absorption of the specimens during the corrosion reaction in the nuclear reactor was also analyzed to evaluate the hydrogen pick-up capability of the Zircaloy-4 cladding tube.

2. Experimental Procedure

The specimens of the Zircaloy-4 cladding tube for this study were taken from the M4 fuel rod in the G23 nuclear fuel rod assembly which was burned for 4 cycles (reload core: 4,5,6,7 cycle, burned core position: A8 → A8 → B7 → B7) in Kori Unit 1. The average burnup of the G23 assembly was 35.5 GWD/MTU and the maximum burnup of the M4 fuel rod was 39.352 GWD/MTU. Fig. 1 shows the intensity profile from γ-scanning along the full length of the M4 fuel rod. The burnup history of the fuel rod suggests that it has a maximum intensity at about

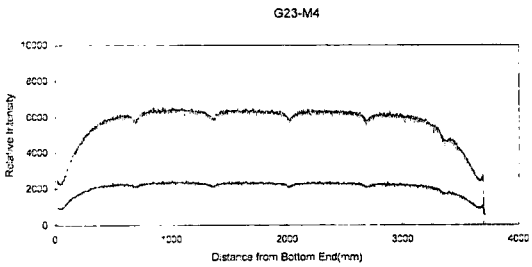

Fig. 1. Gamma Spectrum of the Irradiated Zircaloy-4 Fuel Cladding

40 GWD/MTU. To evaluate the effect of burnup on the rod, the specimens were taken from the two different points near the bottom section of the rod. The analyses based on the γ-scanning showed that the burnup of the two specimens was 18 and 42 GWD/MTU, respectively and the neutron fluence was also about 3.7×10^{21} and 8.0×10^{21} n/cm^2, respectively. The Un-irradiated cladding tube for Kori 1, which was manufactured in the same batch as the irradiated one, was used as a reference specimen for the analyses.

One specimen having a 18 GWD/MTU burnup history and the other one having 42 GWD/MTU were taken from the M4 fuel rod to observe the optical microstructure and they were chemically etched with the solution of 50% H_2O-45% HNO_3-5% HF following auto-polishing using a manipulator in the hot-cell. The optical observation was done on the specimens with UO_2 fuel. The oxide thickness on the specimens was averaged after measuring every 90° direction from the center of the cutting section.

The hardness of the specimens was measured using the Micro-Vickers hardness tester. The values were averaged after many measurements to reduce their errors.

One 6 mm-length specimen having a 18 GWD/MTU burnup and another 6 mm-length specimen having 42 GWD/MTU were taken from the longitudinal direction of the M4 fuel rod to observe the TEM microstructure. The oxide on the exterior and interior surface of the specimens was removed mechanically using a specially designed tool. The thin foil having about a 70μm thickness for TEM observation was made by twin-jet polishing using a solution of 90% ethanol and 10% perchloric acid following chemical polishing of the oxide-removed specimens using a solution of 50% H_2O-45% HNO_3-5% HF after mechanical thinning. During foil thinning an electric current of about 15 voltages flowed to the twin-jet polisher and the temperature of the solution was kept at about -35℃. The microstructure of the thin foil was observed using a TEM (JEOL) operated at 200 kV.

To measure the hydrogen content in the tube before and after irradiation, 5×5 mm^2 specimens were prepared and cleaned sequentially with CCL_4, H_2O and ethanol. The hydrogen content of the specimens was analyzed at the chemical element analysis center of KAERI in accordance with the established procedure.

3. Results and Discussion

3.1. Characteristics of the Un-irradiated Cladding Tube

Fig. 2 shows the TEM microstructure of the un-irradiated stress-relieved Zircaloy-4 cladding tube that was prepared for the reload 4 cycles of Kori Unit 1. The tube had a lot of tangled dislocations and grains with a high dislocation density. The precipitates of 20 nm in size were uniformly distributed in the cold-worked structure of the un-irradiated cladding tube. Stacking faults, which one could typically see in the $ZrCr_2$-type precipitate11), were observed on the precipitate. The precipitate was composed of Fe and Cr and the ratio of Fe/Cr in the precipitate was 1.8 ~ 2.0 and was

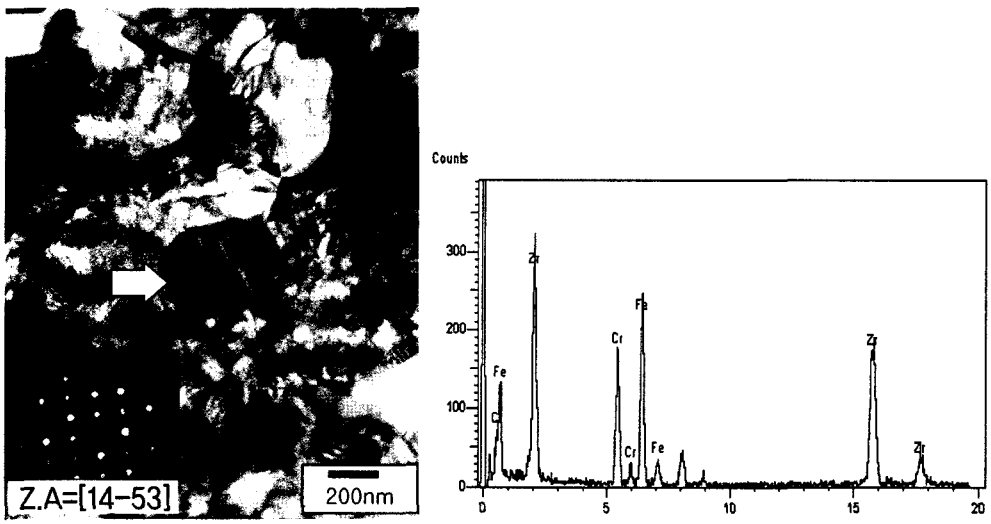

Fig. 2. TEM Microstructures of the Unirradiated Zircaloy-4 Fuel Cladding; (a) Bright field image (b) EDS analysis of ppt

identified as $Zr(Fe, Cr)_2$ which had a C14 Laves phase with a hcp crystal structure.

3.2. Oxidation and Hydrogen Absorption of the Irradiated Tube with Burnup

Fig. 3 shows the optical microstructure of the cutting section of specimen 1. The oxide on the specimen had a very uniform thickness and was dense as well as no noticeable defects. The thickness of oxide was in the range of 5.8 ~ 6.2μm and its average was 6.0μm. Fig. 4 shows that of specimen 2. There are more cracks in the UO_2 pellet of specimen 2 than that of specimen 1. The oxide on specimen 2 was also much thicker than that on specimen 1 since the oxide thickness of specimen 2 was 24 ~ 26.4μm with its average of 25.6μm. That is, to say, the oxide thickness of the Zircaloy-4 cladding tube increased 4.2 times when the burnup increased 2.3 times. The increase of oxide thickness identified in this observation due to the increase of burnup was about 2 times higher than that reported recently for commercial Zircaloy-4 cladding tube[12,13]. Fig. 5 shows the hydride morphologies of specimens 1 and 2. Specimen 2 shows more hydrides than specimen

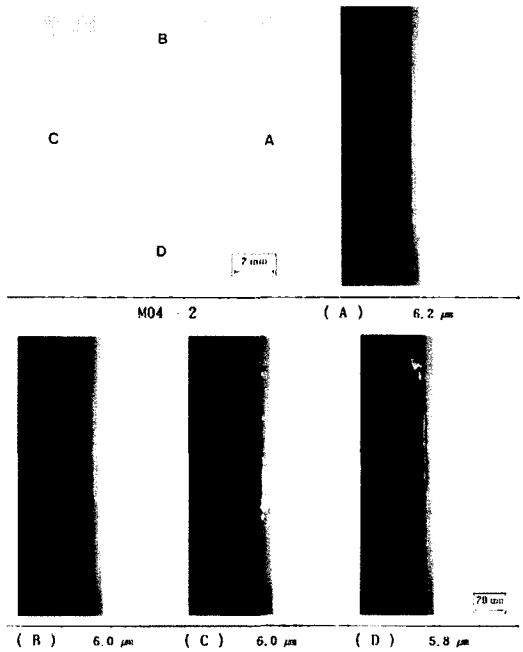

Fig. 3. Optical Microstructures of the Low Burnup Sample (18 GWD/MTU)

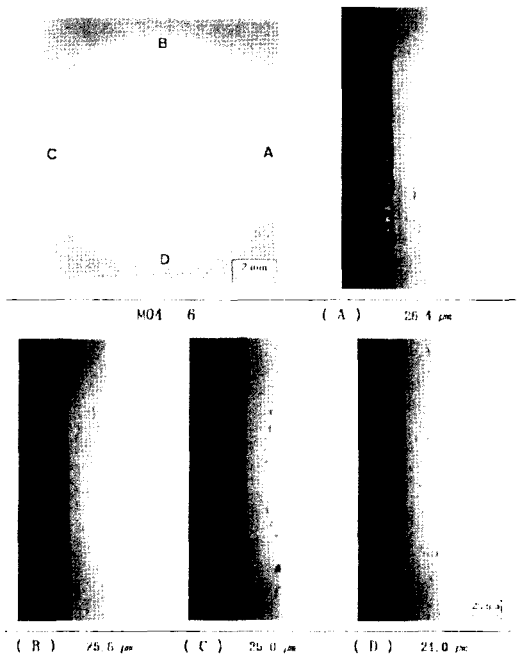

Fig. 4. Optical Microstructures of the High Burnup Sample (42 GWD/MTU)

1 because specimen 2 had a higher burnup history with a longer exposure to a corrosive environment. The hydrogen content in the un-irradiated fuel cladding was 16.2 ppm but that in the irradiated specimen 1 was 54 ppm, and that of the irradiated specimen 2 was 163 ppm. Fig. 6 shows that the hydrogen content in the matrix of the cladding tube increased with the increasing burnup level. Since hydrogen absorption is one of main causes that can lower the mechanical strength of cladding tube, one must consider a way to reduce the hydrogen content in the cladding tube to secure its sound properties. So, many researchers have been trying to develop new cladding tubes that have much less hydrogen content than the Zircaloy-4 tube. One of the recent efforts was an attempt to develop Nb-containing Zr-based alloys for the cladding tube14,15).

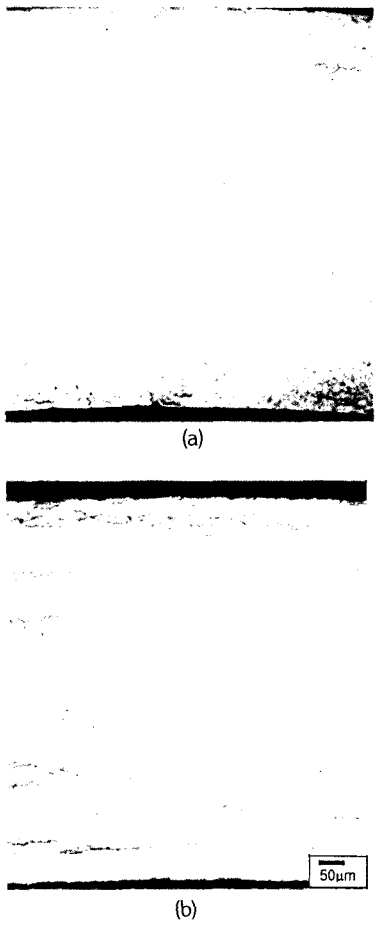

Fig. 5. Hydride Morphologies of the Irradiated Cladding Samples; (a) 18 GWD/MTU (b) 42 GWD/MTU

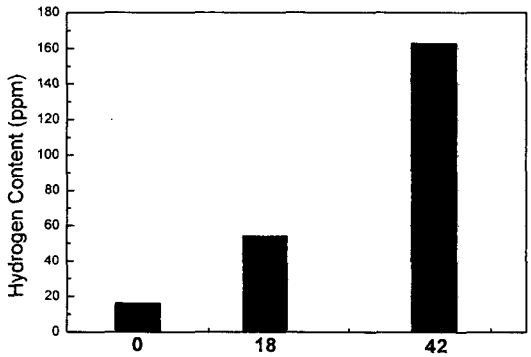

Fig. 6. Hydrogen Contents in the Irradiated Cladding Samples with Burnup

3.3. Hardness Change of the Irradiated Tube with Burnup

Fig. 7 shows the hardness variation of specimens 1 and 2. The irradiation hardening occurred when the burnup was increased. It was difficult to estimate the quantitative increase of the defects in the tube due to irradiation in accordance with the change of burnup history but it was confirmed that a high burnup with irradiation caused an increase of the internal defects giving rise to a hardness increase because the matrix hardness of the irradiated specimen 1 increased by 9.3% and that of the irradiated specimen 2 increased by 24.2%.

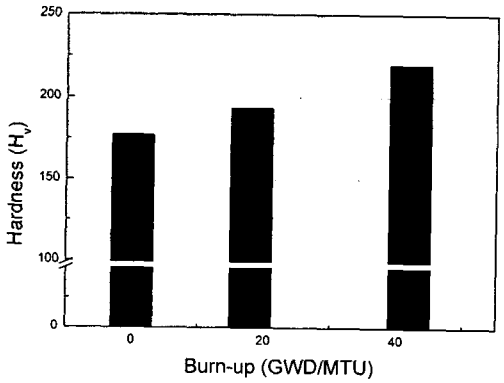

Fig. 7. Hardness Variation in the Irradiated Cladding Samples with Burnup

3.4. Change of Dislocation in the Tube with Burnup

Fig. 8 through 10 shows the TEM microstructures of the irradiated specimens 1 and 2. The two pieces of the picture in Fig. 8 show <a>-type dislocations that were induced in specimen 1 and 2 by irradiation. It is known that <a>-type dislocations can be developed by early irradiation with a relative low fluence of about 1.0 × 10^{20} n/cm^2 [2,3]. It is also reported that the

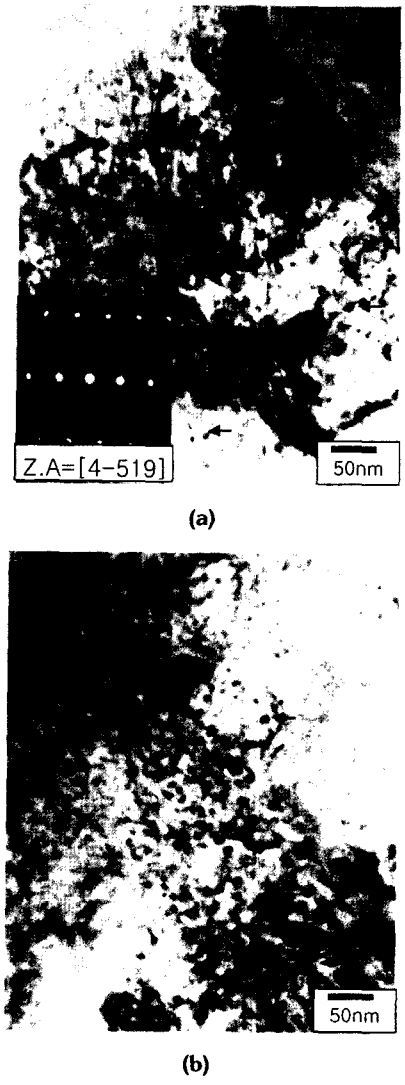

Fig. 8. <a>-type Dislocation Loops in the Burnup Samples; (a) 18 GWD/MTU (b) 42 GWD/MTU

dislocations appear like black spots, and are formed parallel in the [11$\bar{2}$0] direction of the α-Zr with a/3<11$\bar{2}$0> Burgers vector, and their sizes are about 8 nm[3]. The SADP in picture (a) of Fig. 8 shows the pattern of the Zr matrix located at the position that was supposed to be <a>-type dislocation loops[2]. It was found from the calculation that the zone axis of the pattern was

parallel to the $(4\bar{5}19)$ plane. The angle between the $(4\bar{5}19)$ plane and $(11\bar{2}0)$ plane was almost 90°. Therefore, it was confirmed that the dark points indicated by the arrow mark are <a>-type dislocation loops on the $(11\bar{2}0)$ plane. Fig. 8 (b) shows <a>-type dislocation loops which were observed on specimen 2. It can be seen from Fig. 8 that the dislocation density in specimen 2 is higher than that in specimen 1. It is known that the increase of <a>-type dislocation density during early neutron irradiation contributes to the increase of tensile stress[4,5,16,17]. So, it seemed that the hardness of the irradiated tube in the study increased because the density of the <a>-type dislocation loops increased. It is reported that an applied neutron fluence over 4×10^{21} n/cm^2 can cause <c>-type dislocation6,18). As <c>-type dislocation components are merely kinds of vacancies, they can be grown by two-dimensional Fe precipitation that occurs by a way similar to the formation of stacking faults[19]. So, it is known that a lot of Fe can be segregated at the <c>-type dislocations[19]. If the neutron fluence increases, <c>-type dislocation components move their positions by a dislocation climb and can lead to irradiation embrittlement. Fig. 9 shows <c>-type dislocation components observed on specimens 1 and 2. The density of the <c>-type dislocation components in specimen 2 was higher than that of specimen 1 because specimen 2 had more burnup history than specimen 1. <c>-type dislocation components occur as a kind of line on the (0002) basal plane of the α-Zr. <c>-type dislocation components in the specimens were observed in the normal direction of the (0002) plane as shown in Fig. 9. It is known that a <c>-type dislocation component has a close relationship with the growth of the fuel rod. It is also reported that there is a relationship between the formation of precipitate and that of the <c>-type dislocation component[20,21]. The formation

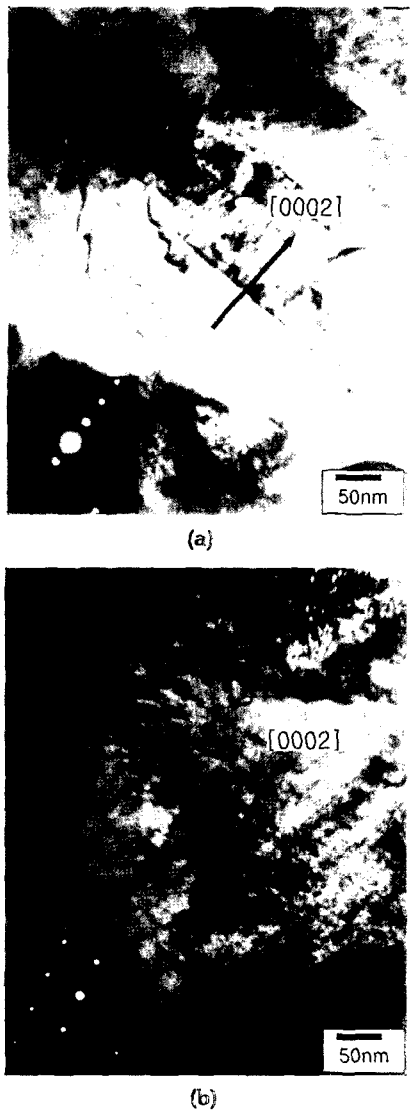

Fig. 9. <c>-type Dislocation Component in the Burnup Samples; (a) 18 GWD/MTU (b) 42 GWD/MTU

and growth of <c>-type dislocation components can make grains contract in the <c> direction in the hcp crystal structure and give rise to the longitudinal growth of the fuel rod[10]. Therefore, it is necessary to study the mechanism systematically for the formation and growth of <c>-type dislocation components.

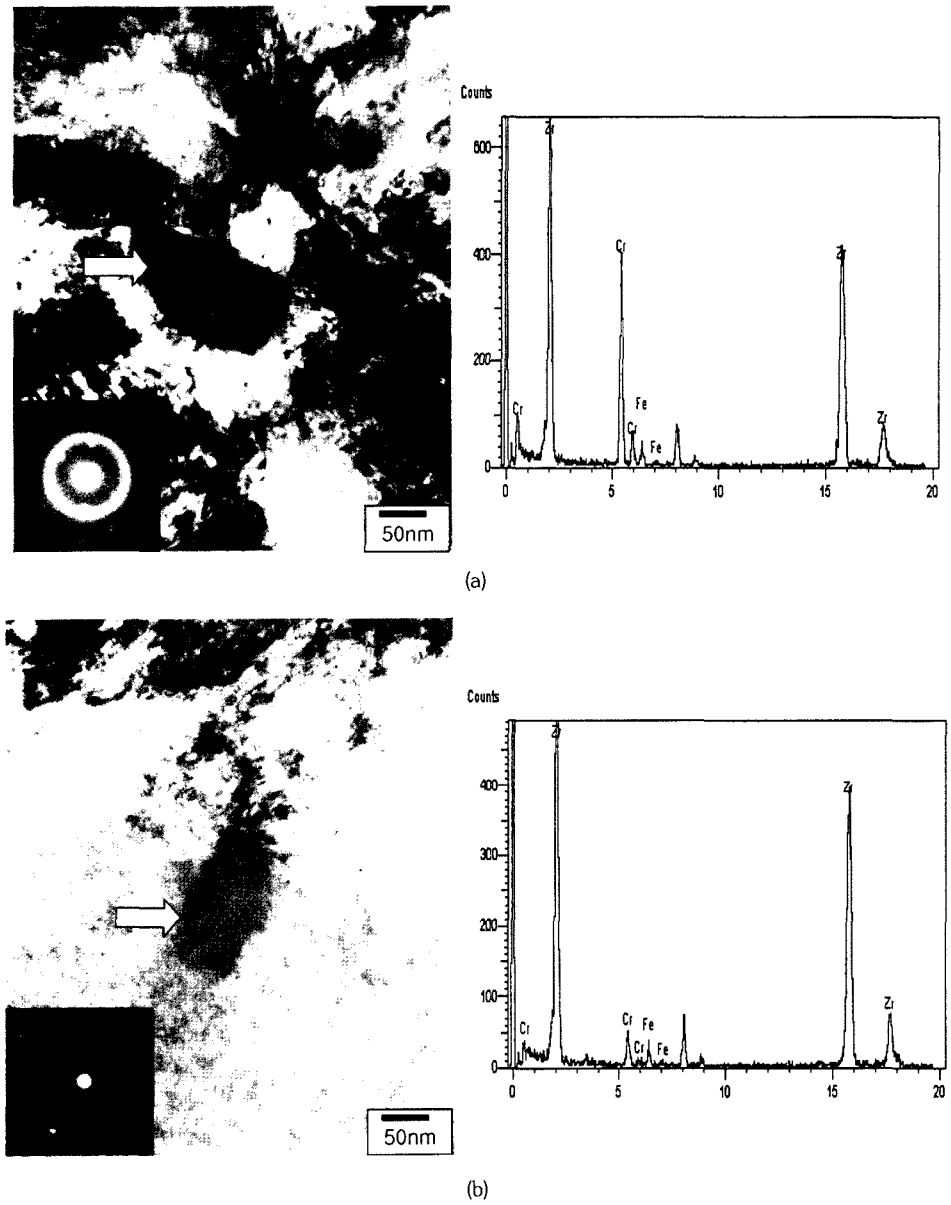

Fig. 10. TEM Image, SAD and EDS Analysis of Amorphous Precipitates in the Burnup Samples; (a) 18 GWD/MTU (b) 42 GWD/MTU

3.5. Amorphous Transformation of Precipitate with Burnup

It is known that the precipitates in Zircaloy-2 and Zircaloy-4 cladding tubes for nuclear fuel rods can be transformed into an amorphous phase when they are irradiated[9,10]. It is also reported that amorphous transformation was sensitive to temperature change and heavily dependent on the neutron flux[22,23]. If precipitates get into an

amorphous transformation, the Fe content in the precipitates can be sharply reduced and the amorphous transformation can be progressed in a linear proportion to the neutron fluence[24]. The fuel rod burnup of 5~15 MWD/MTU (equivalent to about $1\sim4 \times 10^{21}$ n/cm^2) was able to create the precipitates under 20 nm in the cladding dissolve and those over 20 nm get into an amorphous transformation due to neutron irradiation. Amorphous transformation in the M4 fuel rod also occurred as shown in Fig. 10 (a) and (b). The size of precipitates with the kind of amorphous phase was over 100 nm. It was found that the size and observation frequency of the precipitates had a tendency to be reduced with a burnup increase. It might be that the relatively small precipitates had already been dissolved due to the greater progress of the amorphous transformation. It was also found that the amorphous transformation of the precipitates had have been further progressed since almost all the precipitates in the amorphous transformation showed the ring-type diffraction pattern. The amorphous transformation behavior is thought to be an incoherent phenomenon within the crystal structure of the precipitate because the diffusion of Zr and Cr in the precipitate into the matrix is slow while that of Fe is fast due to irradiation[19]. It is known from the EDS analysis that the Fe content in the precipitate was much reduced with the SAD pattern being round indicating an amorphous structure as shown in Fig. 10 (a). The recrystallization of the matrix was observed near the area where the precipitate in specimen 2 was transformed into the amorphous structure. The matrix would have been recrystallized because the Fe element in a precipitate might be diffused around the precipitate by irradiation[24,25]. The content of Fe and Cr in the precipitate, which was beginning the amorphous transformation, was analyzed the applying the EDS method. The ratio of Fe/Cr was calculated to be a very low value 0.10 ~ 0.17. So, it was found that the drastic reduction of Fe content in the amorphous precipitate had a close relationship with Fe diffusion.

3.6. Future Plan

Up to now, the microstructural characteristics of the nuclear fuel cladding which has been used or prepared for the Kori Unit 1 nuclear power plant has been evaluated. The evaluation has been done in nuclear industries in advanced counties but was first tried successfully with this study in Korea. So, the physical properties and integrity of the irradiated fuel cladding could be evaluated in the future in Korea as well as the causes and effects of problems regarding irradiated fuel cladding could also be identified. Therefore, the next study in Korea of irradiated fuel cladding could be focused on identifying what makes in-pile oxidation accelerate.

4. Conclusions

1) When the burnup of the fuel rod M4 in the fuel rod assembly G23 for the Kori Unit 1 nuclear power plant increased from 18 to 42 GWD/MTU, the oxide thickness of the irradiated fuel cladding increased from 6.0(m to 25.3μm with a rapid increase of hydrogen pick-up.
2) The hardness of the fuel cladding (specimen 1) having a 18 GWD/MTU burnup history increased by about 9.3% from that of the cladding having no burnup history as well as that, the hardness of the fuel cladding (specimen 2) having a 42 GWD/MTU burnup history increased by about 24.2%.
3) Both <a>-type dislocation loops and <c>-type dislocation components were observed on the

specimens 1 and 2 which had been irradiated. The density of dislocation loops increased by increasing the fuel rod burnup.

4) The amorphous transformation of the precipitate was observed on the irradiated specimens and its tendency for transformation increased with increased burnup. It seems that the transformation occurred because the Fe element in the precipitate had diffused fast. The ratio of Fe/Cr in the amorphous precipitate was reduced to 0.10 ~ 0.17 and the matrix near the precipitate was recrystallized.

Acknowledgement

This study has been carried out under the nuclear R & D program by MOST.

5. References

1. S.N. Buckley, Proc. Int. Conf. on Properties of Reactor Materials and the Effects of Radiation Damage, Ed. D.J. Littler 413, (Butterworths, London, 1962).
2. D.O. Norhwood, Atomic energy review, 15. 4. (1997) p. 547.
3. D.O. Northwood, R.W. Gilbert, L.E. Bahen, P.M. Kelly, R.G. Blake, A. Jostsons, P.K. Madden, D. Faulkner, W. Bell and R.B. Adamson, J. Nucl. Mater., 379, 79 (1979).
4. M.A. Griffiths, J. Nucl. Mater., 190, 159 (1988).
5. M.A. Griffiths, J. Nucl. Mater., 225, 205 (1993).
6. M.A. Griffiths and R.W. Gilbert, J. Nucl. Mater., 169, 150 (1987).
7. S.R. Mcewen, J. Faber, A.P. Turner, Acta. Metall., 657, 5 (1983).
8. R.A. Holt, J. Nucl. Mater., 310, 159 (1988).
9. R.W. Gilbert, M.A. Griffiths, G.J.C. Carpenter, J. Nucl. Mater., 265, 135 (1985).
10. W.J.S. Yang, R.P. Tucker, B. Cheng, and R.B. Adamson, J. Nucl. Mater., 185, 138 (1986).
11. D. Charquet, E. Alheritiere, "Second phase particles and matrix properties on Zircaloys", Proc. Workshop on second phase particles in Zircaloys, Erlangen FRG, Kern Tech. Gesell. (1985) P. 5.
12. J.P. Mardon, D. Charquet, and J. Senevat, Proc. Of Int. Topical Mtg. on Fuel Performance, West Palm Beach, ANS, La Grange Park, ILL. 646, (1994).
13. L.F. Van Swam, F. Garzarolli, and E. Steiberg, Proc. Of Int. Topical Mtg. on Fuel Performance, West Palm Beach, ANS, La Grange Park, ILL. 303, (1994).
14. J.P. Mardon, D. Charquet, and J. Senevat, Zirconium in the Nuclear Industry, ASTM STP 1354, 505, (2000).
15. P.V. Shebaldov, M.M. Peregud, A.V. Nikulina, Y.K. Bililashvili, A.F. Lositski, N.V. Kuz' menko, V.I. Belov, and A.E. Novoselov, Zirconium in the Nuclear Industry, ASTM STP 1354, 545, (2000).
16. C. Hellio, C. H. De Novion, and L. Boulanger, J. Nucl. Mater., 368, 159 (1988).
17. S.N. Buckley, R. Bullough, and M.R. Hayns, J. Nucl. Mater., 283, 89 (1980).
18. R.A. Holt, M.A. Griffiths, and R.W. Gilbert, J. Nucl. Mater., 51, 149 (1987).
19. Y. De Carlan, C. Regnard, and M.A. Griffths, Zirconium in the Nuclear Industry, ASTM STP 1295, 638, (1996).
20. R.A. Holt, A.R. Causey, and M.A. Griffiths, Zirconium in the Nuclear Industry, ASTM STP 1354, 86, (2000).
21. R.A. Holt and A.R. Causey, J. Nucl. Mater., 1, 28 (1968).

22. A. Motta and C. Lemaignan, J. Nucl. Mater., 277, 195 (1992).
23. D. Pecheur, F. Lefebure, A. Motta, C. Levaignan, and D. Charquet, J. Nucl. Mater., 445, 205 (1993).
24. P.Y. Haung, S.T. Mahmood, and R.B. Adamson, Zirconium in the Nuclear Industry, ASTM STP 1295, 726, (1996).
25. A.V. Nikulina, Y.K. Bililashili, P.P. Markelov, M.M. Peregud, V.A. Kotrekhov, A.F. Lostisky, N.Y. Kuzmenko, Y.P. Shevnin, V.K. Shamardin, G.P. Kobylyansky, and A.E. Nivoselov, Zirconium in the Nuclear Industry, ASTM STP 1295, 785, (1996).